Unique growth strategy in the Earth's first trees revealed in silicified fossil trunks from China

Hong-He Xu[a,1], Christopher M. Berry[b,1], William E. Stein[c,d], Yi Wang[a], Peng Tang[a], and Qiang Fu[a]

[a]State Key Laboratory of Palaeobiology and Stratigraphy, Nanjing Institute of Geology and Palaeontology, Chinese Academy of Sciences, Nanjing 210008, China; [b]School of Earth and Ocean Sciences, Cardiff University, Cardiff CF10 3AT, United Kingdom; [c]Department of Biological Sciences, Binghamton University, Binghamton, NY 13902-6000; and [d]Paleontology, New York State Museum, Albany, NY 12230

Edited by Peter R. Crane, Oak Spring Garden Foundation, Upperville, Virginia, and approved September 26, 2017 (received for review May 21, 2017)

Cladoxylopsida included the earliest large trees that formed critical components of globally transformative pioneering forest ecosystems in the Mid- and early Late Devonian (ca. 393–372 Ma). Well-known cladoxylopsid fossils include the up to ∼1-m-diameter sandstone casts known as *Eospermatopteris* from Middle Devonian strata of New York State. Cladoxylopsid trunk structure comprised a more-or-less distinct cylinder of numerous separate cauline xylem strands connected internally with a network of medullary xylem strands and, near the base, externally with downward-growing roots, all embedded within parenchyma. However, the means by which this complex vascular system was able to grow to a large diameter is unknown. We demonstrate—based on exceptional, up to ∼70-cm-diameter silicified fossil trunks with extensive preservation of cellular anatomy from the early Late Devonian (Frasnian, ca. 374 Ma) of Xinjiang, China—that trunk expansion is associated with a cylindrical zone of diffuse secondary growth within ground and cortical parenchyma and with production of a large amount of wood containing both rays and growth increments concentrically around individual xylem strands by normal cambia. The xylem system accommodates expansion by tearing of individual strand interconnections during secondary development. This mode of growth seems indeterminate, capable of producing trees of large size and, despite some unique features, invites comparison with secondary development in some living monocots. Understanding the structure and growth of cladoxylopsids informs analysis of canopy competition within early forests with the potential to drive global processes.

evolution | Devonian | forests | Cladoxylopsida | plant development

One of the key episodes in the history of the Earth is "afforestation," the Devonian transition to a forested planet (1)—that is, the development of tree-sized vegetation leading to step changes in the behavior of sediment on flood plains, clay mineral production, weathering rates, CO_2 drawdown, and the hydrological cycle (2, 3). In many ways, this event represents perhaps the most fundamental change in Earth system dynamics between the truly ancient and modern.

The fossil record strongly indicates that the origin of trees was not a solitary evolutionary innovation confined to a single clade. Cladoxylopsid trees appeared first (4) [early Mid-Devonian (Eifelian), 393–388 Ma], followed by archaeopteridalean and lycopsid trees [late Mid-Devonian (Givetian), 388–383 Ma] (5, 6). *Archaeopteris*, an early lignophyte, has the most familiar tree growth strategy, exhibiting extensive secondary development by producing secondary xylem (wood) laid down in concentric growth increments by a cylindrical bifacial vascular cambium (7, 8). Lycopsids produced limited secondary xylem and expanded their trunk diameter largely by extensive periderm production (9).

Anatomically well-preserved cladoxylopsids known to date, including *Pietzschia* from the Late Devonian (Famennian, 372–359 Ma) of Morocco (10, 11), probably indicate a primary thickening meristem capable of forming a primary body (and therefore trunks) up to 160 mm across, but demonstrate no secondary increase in diameter. Such plants were likely determinate in growth and limited in size. However, *Eospermatopteris* bases (12) from the older, Mid-Devonian (ca. 385 Ma) in situ Gilboa fossil forest (New York) (13), reached basal diameters of 1 m supporting long tapering trunks (14). The sandstone casts (Fig. 1) reveal coalified vascular strands but only a little preserved cellular anatomy. Thus, despite fragmentary evidence that radially aligned xylem cells in some partially preserved cladoxylopsid fossils may indicate a limited form of secondary growth (4, 7, 11, 15, 16), it remains unclear how this type of plant dramatically increased its girth. We present here exceptionally preserved large trunks from China (Figs. 2 and 3) that demonstrate direct evidence of how these earliest trees were able to expand their trunk diameter and thereby achieve tree size.

Results

Cladoxylopsida

Xinicaulis lignescens gen. et sp. nov. Xu, Berry et Stein

Diagnosis. Trunk bases with large numbers of individual cauline xylem strands in two concentric, closely spaced alternating cylinders: attached inward to anastomosing network of medullary xylem strands and outward to multiple adventitious roots departing downward from sides of cauline strands; all embedded in parenchyma; extensive central pith in larger trunks; individual cauline strands compose primary xylem with concentric secondary xylem including rays and growth increments; primary xylem strand of roots terete in transverse section proximally becoming stellate; secondary xylem also present in medullary strands and roots.

Etymology. *Xin* referring to Xinjiang and meaning "new" in Mandarin; *caulis* Latin, stem; *lignescens* Latin, becoming woody.

Holotype. PB22119 (Fig. 3*A*).

Significance

The evolution of trees and forests in the Mid–Late Devonian Period, 393–359 million years ago, profoundly transformed the terrestrial environment and atmosphere. The oldest fossil trees belong to the Cladoxylopsida. Their water-conducting system is a ring of hundreds of individual strands of xylem (water-conducting cells) that are interconnected in many places. Using anatomically preserved trunks, we show how these trees could grow to a large size by the production of large amounts of soft tissues and new wood around the individual xylem strands and by a controlled structural collapse at the expanding base. We have discovered a complex tree growth strategy unique in Earth history, but with some similarity to that of living palms.

Author contributions: H.-H.X., Y.W., P.T., and Q.F. made initial discovery; H.-H.X., Y.W., P.T., and Q.F. did fieldwork; H.-H.X. and Y.W. did geological interpretation; H.-H.X. and C.M.B. designed research; H.-H.X., C.M.B., W.E.S., Y.W., P.T., and Q.F. performed research; H.-H.X., C.M.B., and W.E.S. analyzed data; and H.-H.X., C.M.B., and W.E.S. wrote the paper.

The authors declare no conflict of interest.

This article is a PNAS Direct Submission.

[1]To whom correspondence may be addressed. Email: berrycm@cf.ac.uk or hhxu@nigpas.ac.cn.

This article contains supporting information online at www.pnas.org/lookup/suppl/doi:10.1073/pnas.1708241114/-/DCSupplemental.

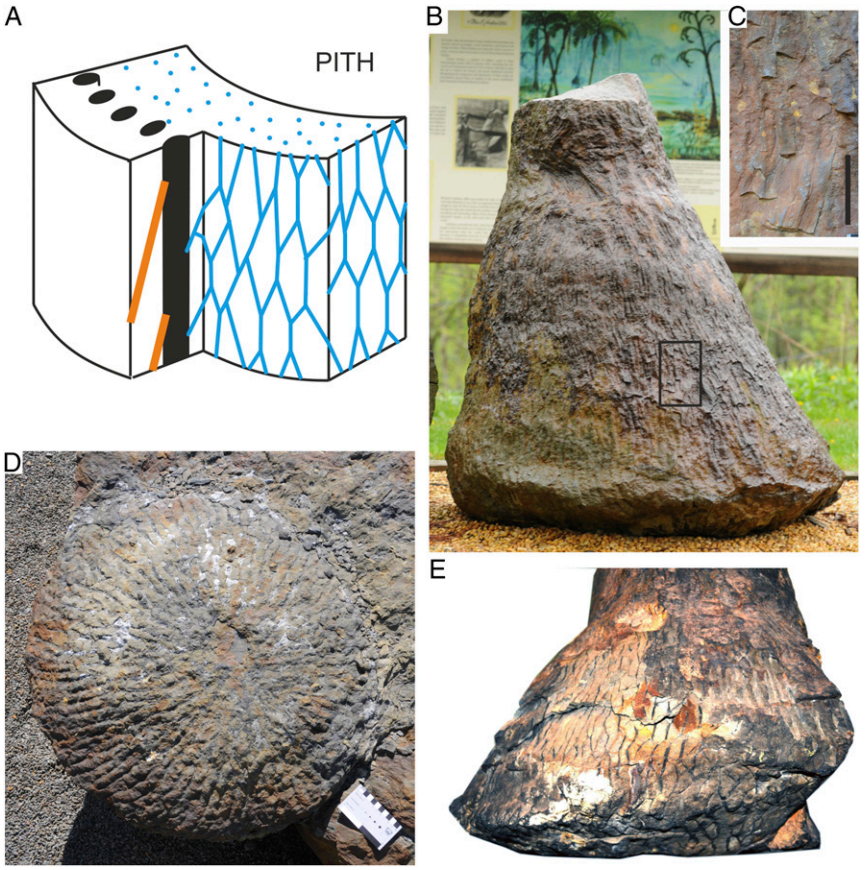

Fig. 1. Vascular system of *Eospermatopteris* from the Middle Devonian of Gilboa, NY. (*A*) Schematic representation of the vascular system based on our observations of the large sandstone trunk casts with largely coalified xylem. By analogy with *Xinicaulis*, black indicates cauline xylem strands, blue indicates medullary xylem strands, and orange indicates adventitious roots. The principal difference between this system and that of *Xinicaulis* is that the cauline xylem strands are apparently arranged in a single, not double, cylinder. (*B*) Lateral view of large specimen on display at the roadside in Gilboa, NY, showing overall form, longitudinal parallel cauline xylem strands, and casts of roots on surface. Basal diameter: ~1 m. (*C*) Close up view of the rectangle indicated in *B*, showing proximal parts of roots emerging from the surface of the cast. (Scale bar, 50 mm.) (*D*) Basal view of upturned stump on open air display at Gilboa Museum, showing outward-dichotomizing cauline xylem strands in base. (Scale bar, 10 cm.) (*E*) Lateral view of specimen on display at Blenheim-Gilboa Visitors Center, North Blenheim, NY, showing internal network of medullary xylem strands exposed on the sides and underneath. Diameter of base: ~50 cm.

Other material. Two blocks from a 70-cm-diameter trunk, PB22120, PB22121 (Fig. 3*B* and Fig. S1*A*).

Locality, age, and horizon. Bulongguoer Reservoir, Hoxtolgay Town, Xinjiang, Northwest China. Loose blocks, volcaniclastic Zhulumute Formation, Frasnian (Late Devonian) (17) (Fig. S2).

Xinicaulis is distinct from *Eospermatopteris* (12) because the cauline xylem strands form a double cylinder rather than a single cylinder.

Our observations are based on two key specimens. The smaller (Fig. 3*A*), prepared as serial sections (Fig. 4 and Fig. S3), has 29–38 individual cauline xylem strands forming a ring in transverse section ~80 mm in diameter, surrounded by a zone of roots in cortical parenchyma up to 32 mm thick, preserved over a length of 100 mm. The larger is a 70-cm-diameter trunk (Figs. 2 and 3*B* and Fig. S1*A*) tapering upward, with the zone of roots up to 10 cm thick, indicating a cylinder of cauline strands of ~50 cm in diameter (Fig. S1*B*).

Primary xylem strands consist of radially directed plates averaging 0.65 mm (small specimen, Fig. 5*E*) and 2.2 mm (large specimen) in radial extent and ~0.2 mm tangentially. In transverse section, polygonal primary xylem cells are surrounded by up to 17 concentric increments of secondary xylem (Fig. 5 *D* and *E*). Tracheids of secondary xylem are thick-walled and square to rectangular in transverse section with conspicuous pit canals (Fig. 5*F*). Growth increments in the secondary xylem have up to 13 cells in each file (Fig. 5*E*). Uniseriate rays (Fig. 5 *G* and *H*), including some with ray tracheids (Fig. 5*I*), are present. In the large specimen, cauline xylem strands consisting of both primary and secondary xylem average 12.4 mm tangentially, with impressive evidence of large secondary expansion (Fig. 5*D*).

In the smaller trunk, the number of cauline xylem strands increases distally by branching, indicating an obconical primary body (Fig. S4). Primary xylem plates are observed to divide radially (Figs. 3*A*, *S*, and 5*A*), but resultant strands become situated in an oblique fashion distally, taking on an alternate arrangement in two concentric cylinders (Fig. 3*A*). We interpret this specimen to represent the trunk very near its base showing upward increasing size and complexity of the primary body (epidogenetic growth), similar in this way to that previously demonstrated for the base of *Pietzschia* (18). The large specimen appears part of a trunk with an estimated ~130 cauline xylem strands (Fig. S1*B*). This specimen likely represents a more distal part of the basal trunk, where the

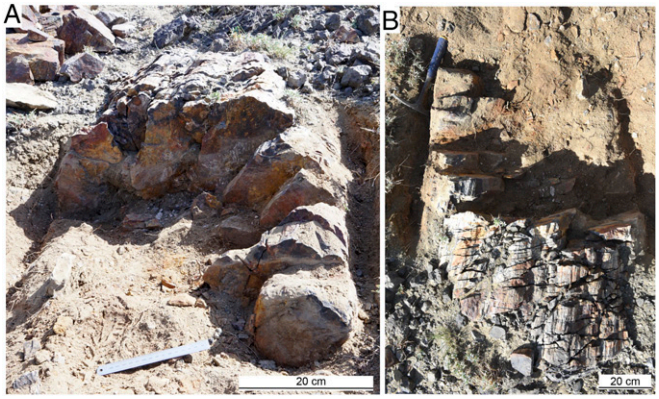

Fig. 2. *X. lignescens* gen. et sp. nov. from the Upper Devonian of Xinjiang, Northwest China. The largest silicified trunk in the field, with a maximum diameter of ~70 cm. Pieces PB22120 and PB22121 collected from this trunk were cut into serial slices. (*A*) Oblique transverse view. (*B*) Lateral view. The trunk is about 1 m long in preserved length.

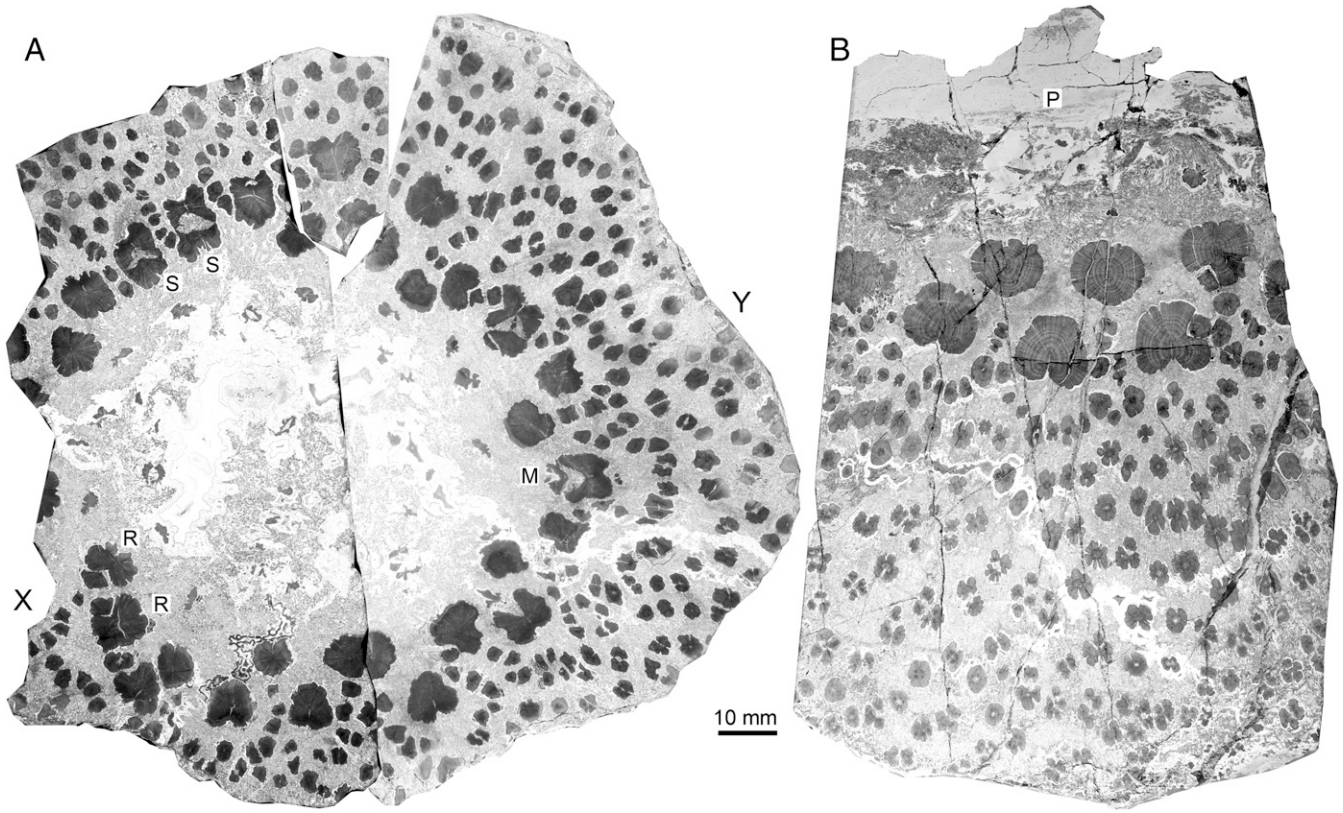

Fig. 3. *X. lignescens* gen. et sp. nov. from the Upper Devonian of Xinjiang, Northwest China. (*A*) Illustrative transverse plane through the small trunk, showing the three naturally fractured parts. Note at least 33 cauline xylem strands forming a double cylinder, some in the process of dividing (*S*), emitting adventitious roots (*R*), or emitting medullary strands (*M*). About 30 medullary xylem strands, of irregular shape, are visible in the almost intact pith. For 3D structure, prepared slices, and strand numbering, see Fig. 4 and Fig. S3. Holotype: PB22119. (*B*) Transverse slice of the outer region of the large trunk (70-cm diameter; see Fig. 2) showing the exterior roots in parenchyma, eight cauline xylem strands, medullary strands in pith parenchyma, and a sediment-infilled pith cavity (*P*). PB22120.

number of primary xylem plates had increased by further divisions during primary growth.

There is abundant evidence of subsequent modification of the primary body through extensive dilatation (19, 20), or diffusely distributed, growth. Below and above the dichotomies of primary xylem plates, normal concentric growth of secondary xylem around the primary xylem plates is observed (Fig. 6*B*, levels *B1* and *B4*). At the level of the more-or-less equal dichotomy, subplates of the primary xylem are often separated by 2–3 mm, with parenchyma and new files of secondary xylem filling the space between them (Figs. 5*A* and 6*B*, level *B2*). The parenchyma cells are notably elongated in the direction of subplate separation, indicating relative tension (21) in the tissue between subplates (Figs. 5 *A* and *B* and 6*F*). At the same level, the outer surface of the cauline strand, presumably the position of the vascular cambium, remains intact (Figs. 5*A*, 6*B*, level *B2*, and 6 *D*–*F* and Fig. S5*F*).

Medullary xylem strands (Fig. 3*A*, M), which both dichotomize and join with other strands distally, show similar formation of elongate parenchyma under tension, including between distally joined strands (Figs. 5*C* and 6*G*, level *A7r*, and Fig. S6). Medullary substrands often show prodigious numbers of new files of secondary xylem and form irregular shapes (Figs. 3 and 5*C*).

Our interpretation of these observations is that the cauline xylem strands have been physically pulled apart, with resulting splits propagating from the dichotomies and unions both proximally and distally during further development (Fig. 6 *C* and *G*). This is made possible by proliferating parenchyma, for which there is clear evidence, in regions surrounding the strands and substrands. In this context, it is interesting to note that cortical and ground tissue parenchyma between cauline xylem strands show variable tension or compression (Fig. 5*D*), but no systematic crushing of mature primary tissues as might have been expected given the volume of secondary xylem produced (7, 21, 22). All of the evidence therefore strongly suggests that the cauline vascular system and trunk as a whole increased in radial dimension

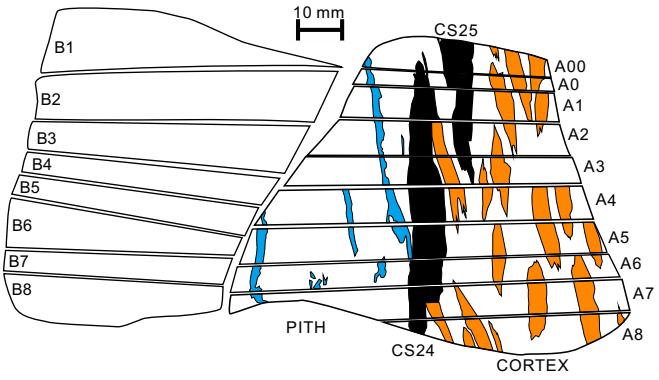

Fig. 4. *X. lignescens* gen. et sp. nov. from the Upper Devonian of Xinjiang, Northwest China. Preparation and general structure of the small trunk specimen (holotype) PB22119. Longitudinal section drawn along the line between *X* and *Y* in Fig. 3*A*, showing slices made in blocks. Face of block A shows cauline xylem strands (black), adventitious roots departing outward and downward (orange), and network of medullary xylem strands connected to the cauline strands (blue).

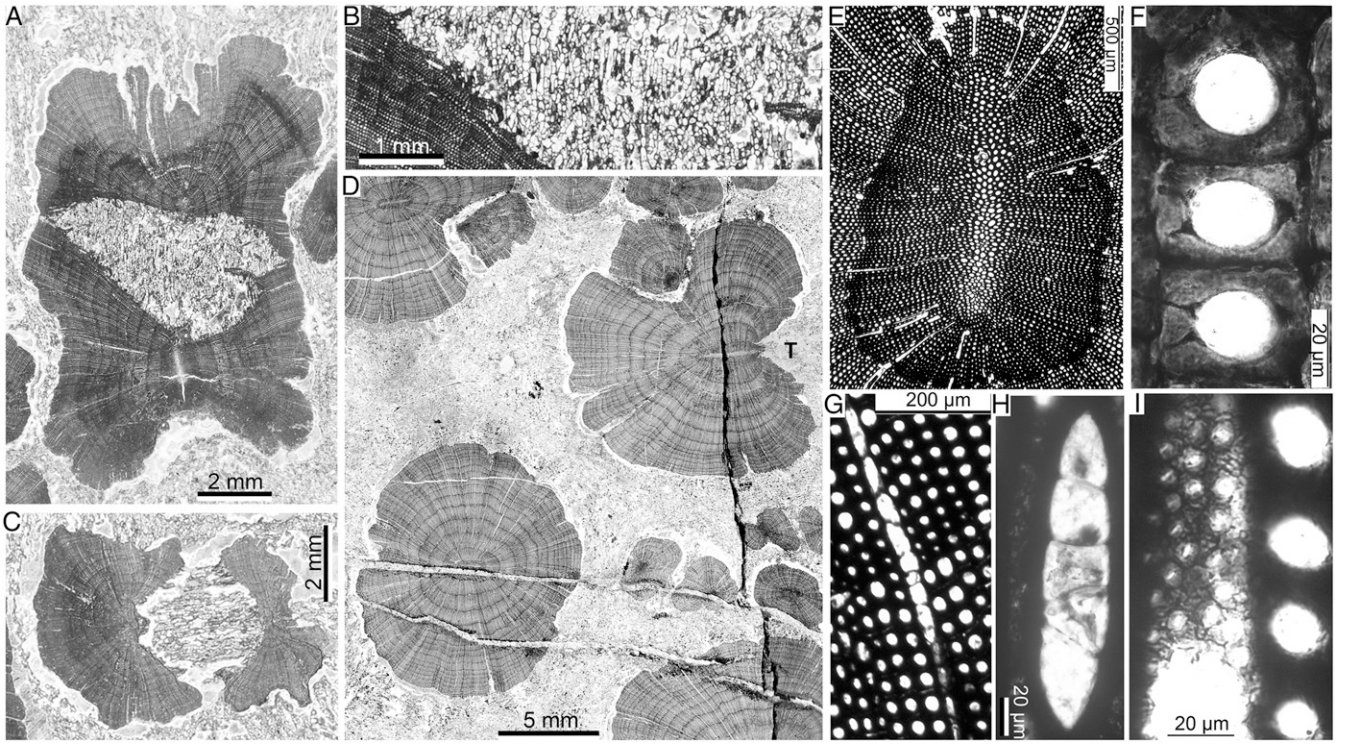

Fig. 5. Transverse and longitudinal sections of *X. lignescens* gen. et sp. nov. from the Upper Devonian of Xinjiang, Northwest China. (*A*) Transverse section of acropetally dichotomizing cauline xylem strand 2 during basipetal splitting. Note profusion of parenchyma cells within split and proliferation of wood via lateral addition of files of secondary xylem at outer margin of developing split. Similar to Fig. 6*B*, slice B2. Outside of trunk is orientated down page. PB22119-B3. (*B*) Enlargement of the left central area of parenchyma in Fig. 5*A* showing pronounced elongation of the cells parallel to separation of the splitting strand and detail of addition of secondary xylem files. (*C*) Acropetal splitting of acropetally joining medullary strands near cauline strand 20, showing secondary growth of xylem and elongation of parenchyma cells. See Fig. 6*G*, slice A7r. Outside of trunk is to the left. For context, see Fig. S6. PB22119-A7. (*D*) Cauline xylem strands from the big trunk showing 17 growth increments around the primary xylem plates, and development of adventitious roots (top) with eccentric growth increments. Note groove on outermost part of cauline strand perhaps representing former position of branch trace (T). Outside of trunk is to the right. PB22120-M2. (*E*) Elliptical primary xylem plate and first growth ring in transverse section of a small trunk, cauline strand 31. PB22119-C2. (*F*) Secondary xylem tracheids in transverse view; radial plane is vertical on page. Note the rectangular outline of each cell, thick walls, and pits on radial walls. PB22119-C2. (*G*) Transverse section of cauline xylem strand 31 with a ray. PB22119-C3. (*H*) Tangential section of a ray five cells high. PB22119-C5. (*I*) Transverse section of cauline xylem strand 31 showing ray tracheid (*Left*). PB22119-C4.

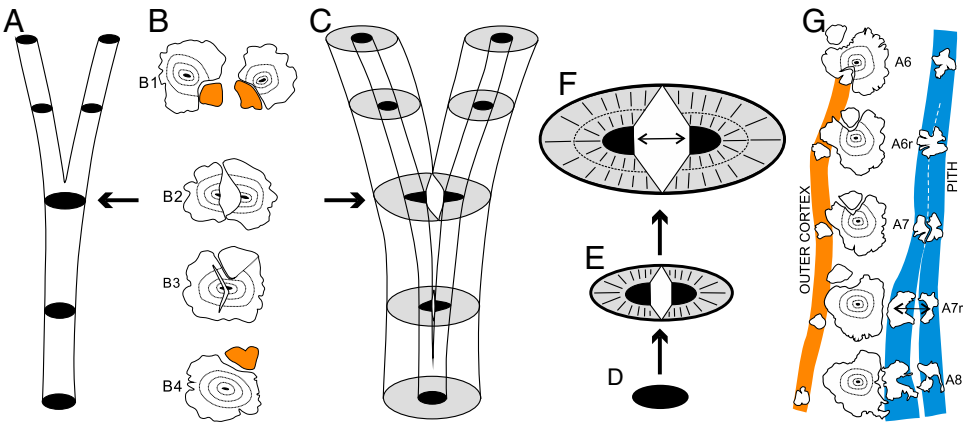

Fig. 6. *X. lignescens* gen. et sp. nov. from the Upper Devonian of Xinjiang, Northwest China. Splitting of xylem strands during enlargement of trunk. PB22119. (*A*) Distally divided cauline primary xylem strand. (*B*) Series through the dichotomy of cauline strand 12 with secondary growth (Fig. S5). (*C*) Interpretation of *B* showing that pulling apart of the daughter xylem strands has caused a crack to be propagated basipetally. Development and proliferation of secondary xylem have kept pace with the splitting at the level of the cambium, but an area of parenchyma has developed under relative tension within the space delimited by the primary and secondary xylem. (*D*–*F*) Developmental history of transverse section of xylem strand at level indicated by arrow in *A*–*C*. (*D*) Primary xylem only. (*E*) One growth increment of secondary xylem. Secondary xylem and vascular cambium have proliferated. (*F*) Further separation. Parenchyma cells developing in gap between the separating halves of the strand show elongation under relative tension in the orientation indicated by double-headed arrow. Black: primary xylem; light gray: secondary xylem; thick black line: vascular cambium. Dashed line: growth increment; white area: parenchyma. (*G*) Series between interconnected medullary strands (blue) and cauline strand 20. Orange: adventitious root. Series drawn from slices A6–A8 (Fig. S6); suffix "r" means bottom of slice, drawing reversed. Thickness of slices ~8 mm, the distance between facing slabs (e.g., A6r–A7) is about 3 mm allowing for saw cut, grinding, and etching. Outer medullary trace shows departure from the cauline strand (A8) and its distal connection with another inner medullary strand (A7). The series shows that the medullary strands are splitting apart acropetally as the inner medullary strand is "pulled" toward the pith, evidenced by the formation and elongation (double-headed arrow) of parenchyma in the gap between the separating strands. The strand continues to split acropetally along a tangentially oriented crack (sections A7–A6r, dashed white line).

over time in a form of secondary development by means of diffuse secondary growth with parenchyma comprising a large proportion or even the bulk of new tissues produced. The increase in distance between the individual cauline and medullary strands caused by this expansion is therefore most manifest at the interconnections, where it can be accommodated only by physical tearing of the xylem. The relative number of interconnections in the medullary xylem strands and their complex topology compared with the cauline strands is likely responsible for the more damaged and irregular appearance of the medullary strands, as they have been subjected to a higher incidence of tearing at the nodes.

Tissues interpreted as phloem were incompletely preserved in small patches next to some xylem strands and have been observed in transverse section only. Some cells are formed in radial files, suggesting a secondary origin. This will be subject to further investigation.

Roots originate adventitiously from the outer and tangential surface of secondary xylem growth increments of the cauline strands (Figs. 3*A*, *R*, 4, 5*D*, and 6*G*), travel steeply down through an outer zone of parenchyma (Fig. 4), frequently divide (Fig. 3), and display growth increments of secondary xylem (Figs. 3 and 5*D*). Primary xylem is small and terete initially, but further from the point of origin becomes increasingly stellate (Fig. 3 and Fig. S1*A*).

Branch traces are not observed. However, many transverse sections of cauline xylem strands show a groove on the outermost surface (Figs. 3 and 5*D*, T) in line with, and as deep as, the primary xylem plate, which may represent disruption to the cambium caused by the presence of branch traces. Evidence of the traces themselves are presumed to have been destroyed at these lower levels by secondary modification of most tissues of the trunk.

Discussion

Our results indicate that the large size of *Xinicaulis* on a scale equivalent to *Eospermatopteris* was accomplished by a unique form of secondary development, facilitated primarily by a long-acting cylindrical zone of diffuse secondary growth in ground and inner cortical tissues of the base and main trunk. Although similar to some monocots in general behavior (23), secondary growth in the stems of *Xinicaulis* did not produce distinctive radial files of parenchyma or additional vascular strands. Instead, continued activity served only to increase overall volume of the stem via mostly unordered parenchyma and created patterned fracturing of the vascular strands at primary xylem dichotomies in both proximal and distal directions. Since increase in tissue volume has important consequences, both physiological and structural, it seems very likely that all cladoxylopsid plants of tree size using this mode of growth of necessity would have a hollow pith (Fig. 3*B* and Fig. S1*B*). In addition, *Xinicaulis* is also associated with an equally unusual form of secondary development in which radial files of secondary xylem are produced by cambia around individual cauline strands, medullary strands, and roots rather than forming a single solid cylinder as generally expected in seed plants. Secondary xylem greatly increased both conductive capacity and support presumably to keep pace with increasing size of the plant during development. It is interesting to note that cell walls of the secondary xylem in *Xinicaulis* are unusually thick, for example, compared with *Callixylon* (the trunk of the progymnosperm tree *Archaeopteris*) from the same locality (Fig. S7), possibly indicating relatively greater importance of support over conductive capacity in a fibrous plant body overall (and suggesting a significant capacity for cladoxylopsids to drawn-down atmospheric carbon).

The manner of secondary development in *Xinicaulis* seems potentially indeterminate and thus capable of producing trees of very large size. This invites close comparison with *Eospermatopteris*, with stumps showing similar size and taper as our largest Chinese specimen and with a similar construction of the xylem system including longitudinal cauline xylem strands, anastomosing medullary xylem strands, central pith, and external adventitious roots (12–14). Fragmentary coalified, but clearly formerly woody, xylem strands have also been found preserved within *Eospermatopteris* casts (Fig. 1). However, unlike in the large Xinjiang *Xinicaulis* specimen, the very bottom of the trunk is clearly represented. Our observations of *Eospermatopteris* suggest the initially upright, upward-dichotomizing, upward-expanding part of the vascular system produced during early development may end up as a radially expanded horizontally almost flattened disk (Fig. 1*D*) in larger trees due to continued lateral diffuse secondary growth combined with longitudinal structural failure with increasing size over time (Fig. 7).

By contrast, other cladoxylopsid trees such as *Pietzschia* so far exhibit only primary growth and retain an intact, partially vascularized pith (10, 11). If representative of determinate development, it seems likely that these examples adopted a tree fern strategy (18) whereby upward increasing complexity and size of the primary body (epidogenesis) was supported by an ever-enlarging root mantle. However, given what we know at this point in time, there is no

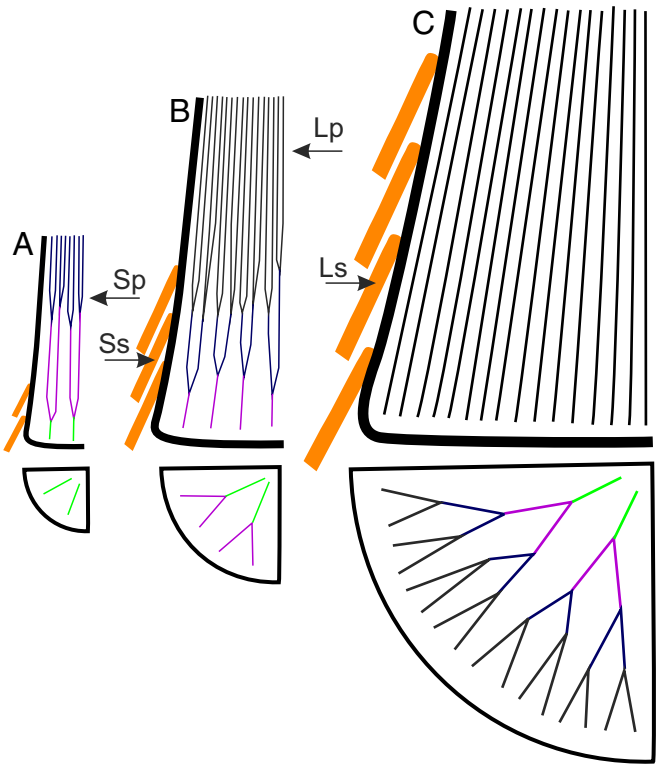

Fig. 7. *X. lignescens* gen. et sp. nov. Schematic model of development showing the position of the blocks describe in this paper. A developmental model showing three growth stages of the trunk in lateral (*Upper*) and basal (*Lower*) view. Colors show primary cauline xylem strands formed in a time series from the growing apex. (*A*) Juvenile stage: the primary body has grown sufficiently to produce about 30 cauline strands by upward dichotomy of individual strands. (*B*) Intermediate stage with further enlargement of the primary body and a maximum number of cauline xylem strands produced (black lines). (*C*) Mature stage with maximum secondary growth of cauline xylem strands to produce large diameter trunk. In this model, suggested here by C. M. Berry and W. E. Stein based on observations on *Eospermatopteris* from New York, the upward-dichotomizing cauline and medullary xylem system is gradually incorporated into the almost flat expanding base (Fig. 1*D*). The alternative, a tree-fern like basal system, as found in *Pietzschia* with primary growth only (18), is considered unlikely in such a large trunk. *Sp* indicates the hypothetical position of the small trunk specimen with largely only primary growth, and *Ss* indicates the position of the same specimen with secondary growth as illustrated in this paper. *Lp* indicates the hypothetical position of the large trunk specimen with largely only primary growth, and *Ls* indicates the position of the large specimen following secondary growth as illustrated in this paper.

reason to preclude intermediate conditions with various degrees of secondary development and a concomitant shift in support strategy.

Most intriguing, perhaps, is the obvious convergence in form and development between *Xinicaulis*, and by implication some other cladoxylopsids, and living tree-form monocot angiosperms, such as palms, to be contrasted with "true" secondary development via a single well-organized vascular cambium as seen in most lignophytes. Although unique in significant respects (production of secondary xylem around each vascular strand via a normal vascular cambium and patterned fracture of the primary xylem architecture during secondary development), the general mode of development of *Xinicaulis* is nevertheless eminently recognizable among modern forms. The model of both primary and secondary development in cladoxylopsids that we propose closely follows a long-standing view by Eckhardt (24; also cited in ref. 19, p. 390), so much so that nothing ad hoc seems necessary. Although strikingly similar, it is also reasonably clear that cladoxylopsids and palms evolved these features independently (7), so an analogy in growth can be carried only so far. However, the fact that palms, *Xinicaulis*, likely *Eospermatopteris*, and, for that matter, at least some cormose tree lycopsids all share significant structural similarities including few apical meristems, a strong central axis, and many roots of nearly equal size (usually termed "rootlets") may indicate what is possible, but perhaps also limiting, in plants of tree size lacking a standard single cylindrical vascular cambium.

Materials and Methods

We predominantly studied thick transverse and longitudinal sections of the silicified trunks. These were cut by saw and then polished by hand on a grinding wheel or on a vibrating lap to give a uniform black finish. The exposed surfaces were etched for 45–90 s in hydrofluoric acid (HF) in a dedicated HF fume hood. Testing of these samples showed that there was no need to pretreat the material in HCl to remove carbonates as none were present. The reaction with HF resulted in the carbonized cell walls being clearly visible against the white frosted silica. The sections were subsequently rinsed in water with the runoff neutralized in supersaturated sodium carbonate solution. After neutralization, the specimens were further washed in running water for several hours and then air-dried. Standard protocols and personal protective equipment for HF work were adopted while handling HF and HF-contaminated specimens. The dry specimens were photographed with a Nikon D800 camera and 60-mm macro lens or Leica M12 microscope. Some small thin sections were ground by hand using traditional techniques to study histological details. They were photographed using a Leica DMR compound microscope and Leica cameras. Measurements were made using Leica LAS software.

All specimens were deposited in the Nanjing Institute of Geology and Palaeontology, Chinese Academy of Sciences, Nanjing, China, with the prefix PB.

ACKNOWLEDGMENTS. This study was financially supported by the Natural Science Foundation of China (Grants 41530103 and 41772012). Natural Environment Research Council Grant NE/J007897/1 (to C.M.B. with W.E.S. as visiting researcher) made possible the collaboration between W.E.S., H.-H.X., and C.M.B., and the parallel study of *Eospermatopteris*.

1. Scheckler SE (2001) Afforestation: The first forests. *Palaeobiology II*, eds Briggs DEG, Crowther PR (Blackwell Science, Oxford), pp 67–71.
2. Morris JL, et al. (2015) Investigating Devonian trees as geo-engineers of past climates: Linking palaeosols to palaeobotany and experimental geobiology. *Palaeontology* 58: 787–801.
3. Davies NS, Gibling MR (2010) Cambrian to Devonian evolution of alluvial systems: The sedimentological impact of the earliest land plants. *Earth Sci Rev* 98:171–200.
4. Giesen P, Berry CM (2013) Reconstruction and growth of the early tree *Calamophyton* (Pseudosporochnales, Cladoxylopsida) based on exceptionally complete specimens from Lindlar, Germany (Mid-Devonian): Organic connection of *Calamophyton* branches and *Duisbergia* trunks. *Int J Plant Sci* 174:665–686.
5. Cornet L, Gerrienne P, Meyer-Berthaud B, Prestianni C (2012) A Middle Devonian *Callixylon* (Archaeopteridales) from Ronquières, Belgium. *Rev Palaeobot Palynol* 183:1–8.
6. Berry CM, Marshall JEA (2015) Lycopsid forests in the early Late Devonian paleoequatorial zone of Svalbard. *Geology* 43:1043–1046.
7. Meyer-Berthaud B, Soria A, Decombeix AL The land plant cover in the Devonian: A reassessment of the evolution of the tree habit. *The Terrestrialization Process: Modelling Complex Interactions at the Biosphere-Geosphere Interface*, eds Vecoli M, Clément G, Meyer-Berthaud B (Geological Society of London, London), Vol 339, pp 59–70.
8. Meyer-Berthaud B, Scheckler SE, Wendt J (1999) *Archaeopteris* is the earliest known modern tree. *Nature* 938:700–701.
9. Meyer-Berthaud B, Decombeix A-L (2009) L'évolution des premiers arbres: les stratégies dévoniennes. *C R Palevol* 8:155–165.
10. Soria A, Meyer-Berthaud B (2005) Reconstructing the Late Devonian cladoxylopsid *Pietzschia schulleri* from new specimens from southeastern Morocco. *Int J Plant Sci* 166:857–874.
11. Soria A, Meyer-Berthaud B, Scheckler SE (2001) Reconstructing the architecture and growth habit of *Pietzschia levis* sp. nov. (Cladoxylopsida) from the Late Devonian of southeastern Morocco. *Int J Plant Sci* 162:911–926.
12. Goldring W (1927) The oldest known petrified forest. *Sci Mon* 24:514–529.
13. Stein WE, Berry CM, Hernick LVA, Mannolini F (2012) Surprisingly complex community discovered in the mid-Devonian fossil forest at Gilboa. *Nature* 483:78–81.
14. Stein WE, Mannolini F, Hernick LVA, Landing E, Berry CM (2007) Giant cladoxylopsid trees resolve the enigma of the Earth's earliest forest stumps at Gilboa. *Nature* 446:904–907.
15. Berry CM, Fairon-Demaret M (1997) A reinvestigation of the cladoxylopsid *Pseudosporochnus nodosus* Leclercq et Banks from the Middle Devonian of Goé, Belgium. *Int J Plant Sci* 158:350–372.
16. Berry CM, Fairon-Demaret M (2002) The architecture of *Pseudosporochnus nodosus* Leclercq et Banks: A Middle Devonian cladoxylopsid from Belgium. *Int J Plant Sci* 163:699–713.
17. Suttner TJ, et al. (2014) Stratigraphy and facies development of the marine Late Devonian near the Boulongour Reservoir, northwest Xinjiang, China. *J Asian Earth Sci* 80:101–118.
18. Soria A, Meyer-Berthaud B (2004) Tree fern growth strategy in the Late Devonian cladoxylopsid species *Pietzschia levis* from the study of its stem and root system. *Am J Bot* 91:10–23.
19. Esau K (1965) *Plant Anatomy* (John Wiley & Sons, Inc., New York), 2nd Ed.
20. Evert RF (2006) *Esau's Plant Anatomy* (John Wiley & Sons, Inc., Hoboken, NJ).
21. Hotton CL, Stein WE (1994) An ontogenetic model for the Mississippian seed plant family Calamopityaceae. *Int J Plant Sci* 155:119–142.
22. Soria A, Rowe NP, Galtier J, Speck T (2006) Having or lacking secondary growth: Consequences on the mechanical architecture of Paleozoic cladoxylopsids (fern-like plants). *Fifth Plant Biomechanics Conference* (STFI Packforsk, Stockholm), pp 43–48.
23. Tomlinson PB (1990) *The Structural Biology of Palms* (Clarendon Press, Oxford).
24. Eckardt T (1941) Kritische untersuchungen über das primäre dickenwachstum bei monokotylen, mit ausblick auf dessen verhältnis zur sekundären verdickung. *Bot Arch* 42:289–334. German.
25. Cai C-Y, Qin H-Z (1986) First *Leptophloeum rhombicum* stem with internal structure from the Upper Devonian of Sinkiang Uighur. *Acta Palaeot Sin* 25:516–524.
26. Cai C-Y (1989) Two *Callixylon* species from Upper Devonian of Junggar Basin, Xinjiang. *Acta Palaeot Sin* 28:571–578.